Microstructure and formation mechanism of titanium matrix composites coating on Ti-6Al-4V by laser cladding

Wei Niu (牛 伟)[1], Ronglu Sun (孙荣禄)[1,2], Yiwen Lei (雷贻文)[1], and Xihua Guo (郭喜华)[1]

[1]*School of Mechanical and Electronic Engineering, Tianjin Polytechnic University, Tianjin 300160*

[2]*Tianjin Area Major Laboratory of Advanced Mechanical and Electronics Equipment Technology, Tianjin 300160*

Received September 16, 2008; revised October 10, 2008

Abstract Titanium matrix composite coatings were fabricated on Ti-6Al-4V substrate by laser cladding using powder mixtures of Ti+Cr_3C_2 and Ti+TiB_2, respectively. The chemical compositions and microstructures of the coatings were analyzed using scanning electron microscope (SEM), energy dispersive spectrometer (EDS) and X-ray diffraction (XRD). Microhardness was measured by a microhardness tester. The results showed that Cr_3C_2 particles were dissolved and deposited to form dendritic TiC in the upper section and spherical grain TiC in the bottom of Cr_3C_2+Ti coating. Most of TiB_2 was dissolved in the molten pool by laser irradiation, then formed TiB with fine needles and coarse needles in the TiB_2+Ti coating. A few quasi-melted TiB_2 particles with irregular shape at the bottom of the coating were observed. The average microhardnesses were approximately HV850—HV1000, HV800—HV1050 in the Cr_3C_2+Ti and TiB_2+Ti coating, respectively, which were $2-3$ times higher than that of Ti-6Al-4V substrate.

Key words laser technique; laser cladding; composites coating; microstructure; mechanism.

CLCN: TG 156.99 Document Code: A doi: 10.3788/CJL20083511.1756.

1. Introduction

Titanium alloy is an excellent material with high ratio of strength to weight, good corrosion resistance, and good toughness, however, it also has some disadvantages of high friction and poor wear resistance. Recently, several attempts have been made to improve the wear resistance of Ti and Ti alloy by laser cladding[1~8]. Ocelík *et al.*[1] injected WC and TiB_2 powders into the laser melted surface of Ti-6Al-4V alloy and observed an increase in wear resistance. Mridha *et al.*[2] demonstrated that the injection of SiC powder into laser surface melted titanium alloys increased the microhardness of the melted zone to HV600~1200. Zhang *et al.*[6] investigated laser clad coating of TiC-Cr_7C_3-Ti-Ni multiphase metal-ceramic composite for improving the comprehensive properties of the material. The results showed that laser cladding could produce metal matrix composite layers with ceramic particles on titanium alloy surface.

Titanium matrix composites (TMCs) with good wear resistance are favorable materials in the aerospace industry. This paper investigates the laser clad TMCs coating on Ti-6Al-4V alloy surface with powder mixtures of Ti+Cr_3C_2 and Ti+TiB_2, and the microstructure, the formation mechanism, and the microhardness of the composites coating.

2. Experiment

Commercial Ti-6Al-4V alloy was used as the substrate with size of 60×20×5 (mm). The chemical composition of the alloy was $5.5 \sim 6.8$Al, $3.4 \sim 4.5$V (mass fraction), and balance Ti. The sample surfaces were polished and smoothed with emery paper and degreased with alcohol. The powder mixtures used as the clad materials were prepared from 25% Cr_3C_2 +75 % Ti, 25% TiB_2+75% Ti (volume fraction). The particle sizes of Ti, Cr_3C_2, and TiB_2 powders were about 50, 40, and 40 μm, respectively. The powder mixtures were pre-placed on the specimen's surface with thickness of 1.0 mm.

Laser cladding was performed on a 5 kW continuous CO_2 laser processing system. The processing parameters were laser power of 2.5 kW, laser beam diameter of 3 mm, scanning speed of 8 mm/s. As titanium alloys were oxidized rapidly in the air at high temperature, argon gas was used as shielding gas during laser cladding process.

Microstructure of the coating was examined with an XJL-02 optical microscopy, and was observed by a QUANTA200 scanning electron microscopy (SEM) with an energy dispersive spectrometer (EDS). Phase identification was carried out on a D8 X-ray diffractometer (XRD) with Cu-Kα radiation operated at 40 kV and 20 mA. Microhardness was measured with a load of 1000 g and a holding time of 15 s by using an HXD-1000 digital microhardness tester.

3. Results and discussion

3.1 Microstructure of coating

Figures 1 and 2 show the surface and cross-section morphologies of the laser clad coatings. The surfaces of coatings are smooth and free from pore and crack, and appears concave with wave. The boundaries of laser clad

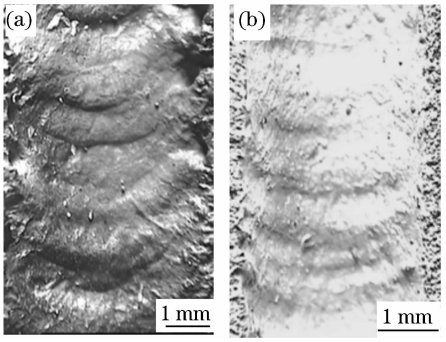

Fig. 1. Surface morphologies of (a) Cr_3C_2+Ti and (b) TiB_2+Ti coatings.

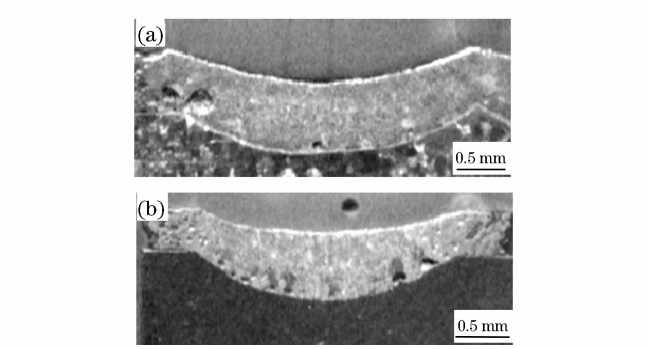

Fig. 2. Cross-section morphologies of (a) Cr_3C_2+Ti and (b) TiB_2+Ti coatings.

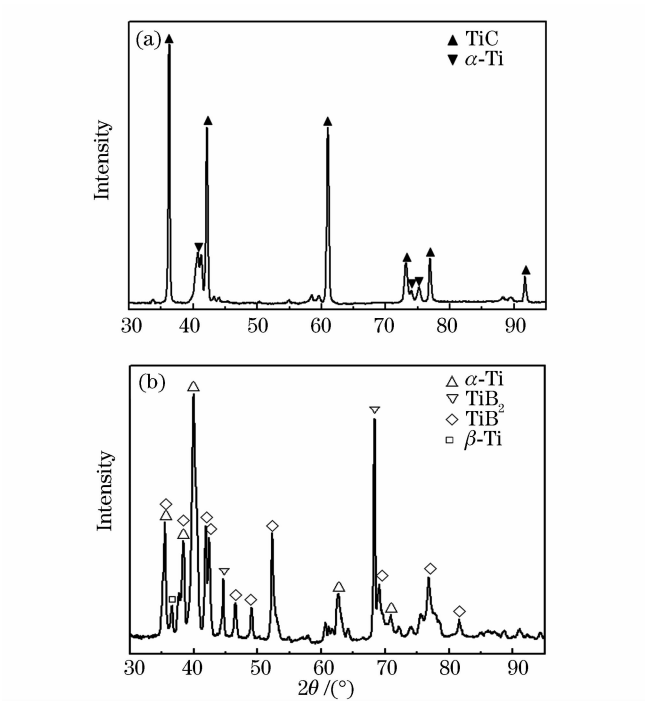

Fig. 3. XRD patterns of laser clad (a) Cr_3C_2+Ti and (b) TiB_2+Ti coatings.

track are approximately smooth (Fig. 1). A few pores exist in the bottom and edge of the coatings (Fig. 2). The width and depth of the Cr_3C_2+Ti coating are 5.1 and 0.8 mm and these of the TiB_2+Ti coating are 4.5 and 0.6 mm, respectively. The depth of the coating is less than that of pre-placed powders, due to partial splash of the pre-placed powders.

3.2 Microstructure and phase analysis

Figures 3(a) and (b) show the XRD spectra of the Cr_3C_2+Ti and TiB_2+Ti coating, respectively. The laser clad Cr_3C_2+Ti coatings consisted of α-Ti and TiC (Fig. 3(a)). The Cr_3C_2 particles entirely disappeared after laser irradiation and the reinforcing phase was TiC only. There are

$$2\mathrm{Ti} + \mathrm{Cr_3C_2} \rightarrow 2\mathrm{TiC} + 3\mathrm{Cr}, \quad (1)$$

$$\mathrm{Ti} + \mathrm{TiB_2} \rightarrow 2\mathrm{TiB}. \quad (2)$$

It indicates that the chemical reaction (1) between the Cr_3C_2 particles and molten Ti might take place and TiC was formed during laser process. Meanwhile, the phase constituents in the laser clad TiB_2+Ti coating are α-Ti, β-Ti, TiB_2 and TiB (Fig. 3(b)). Since the clad material is a mixture of TiB_2 and Ti, TiB is a new phase formed in the coating. The chemical reaction (2) between the TiB_2 particles and molten Ti might take place and TiB was formed.

The SEM micrograph of the Cr_3C_2+Ti coating is shown in Fig. 4. The coatings mainly consist of dendritic and spherical phase. The dendrites are distributed near the surface of coating (Fig. 4(a)). And near the interface of substrate and coating, the reinforcing phase is spherical grain with size of slightly less than 2 μm (Fig. 4(b)). Figure 5 shows the EDS of dendrites and spherical grains. These phases are enriched in Ti and C, which are identified TiC, according to the XRD pattern (Fig. 3(a)). The morphology of TiC particles changes from spherical

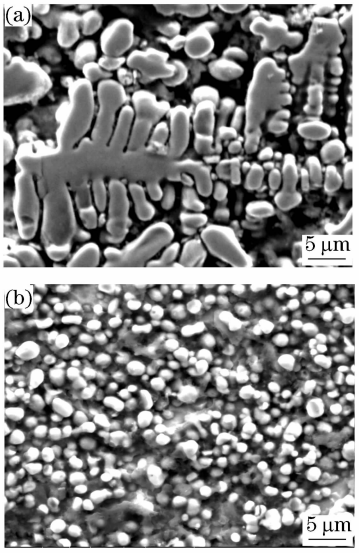

Fig. 4. SEM micrographs of laser clad Cr_3C_2+Ti coating. (a) surface; (b) bottom.

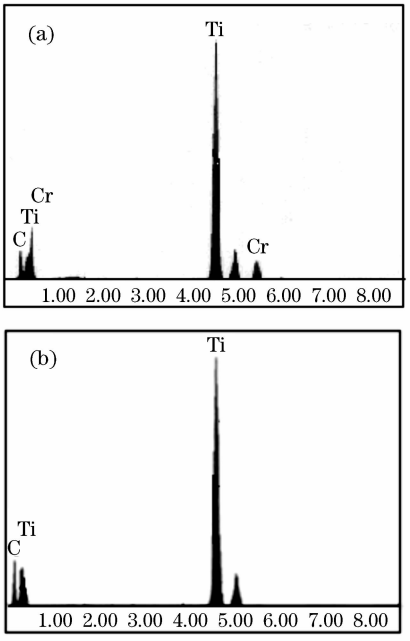

Fig. 5. EDS of different phases of (a) dendrite and (b) spherical grains.

to dendritic shape from bottom to upper section. It is well known that the solidification rate and the liquid temperature gradient at the liquid-solid interface decide the morphology of solid-liquid interface. Generally, in the molten pool the liquid temperature gradient decreases rapidly from the maximum to the minimum, while the solidification rate increases from the minimum to the maximum from the molten pool bottom to its top. Therefore, according to the constitutional supercooling theory, when solidification starts, the solidification takes place in a plane front. In the process, octahedral TiC nuclei precipitates out, and TiC grows to form smaller spherical shape in the bottom of the molten pool. After that, the solidification rate rapidly increases and the temperature gradient decreases rapidly, the microstructure changes into dendrite in the upper section of the coating.

Figure 6 shows the microstructure of the TiB_2+Ti composite coating. Two morphologies can be distinguished, which are needles and irregular particles. In Fig. 6(a), the microstructure is mainly present in the form of coarser needles with diameter and length of 3 and 50 μm, respectively. These coarser structures are found mostly in the surface of the coating. Fine needles have a mean diameter of 200 nm and a length of 15 μm (Fig. 6(b)), which is present in the bottom of the coating. Figure 6(b) also shows quasi-melted particles TiB_2 surrounded by fine needles. The composition of the needles is indicated by EDS analysis (Fig. 7(a)), which is enriched in Ti and B, and the content of B is less than that in quasi-melted particles TiB_2 (Fig. 7(b)). Responding to XRD pattern of the TiB_2+Ti composite coating (Fig. 3(b)), needles are identified TiB. It is believed that under laser irradiation, the temperature of the melting pool may transiently reach a rather high level. Meanwhile, the TiB_2 particles can be achieved at higher temperatures because of its high absorption-coefficient of laser energy and low heat conductivity, thus the partial melting on its boundary occurs. A boron-rich zone is established because of the melting of a TiB_2 particle on its boundary. Considering the large affinity of titanium and boron, the titanium may preferentially react with boron in the melted pool to form TiB.

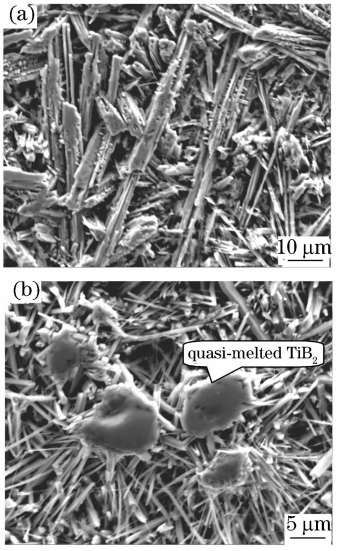

Fig. 6. SEM micrographs of laser clad TiB_2+Ti coating. (a) surface; (b) bottom.

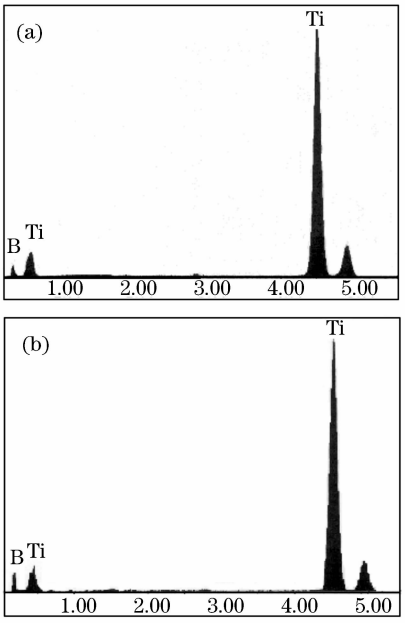

Fig. 7. EDS of different phases. (a) needles; (b) quasi-melted particles TiB_2.

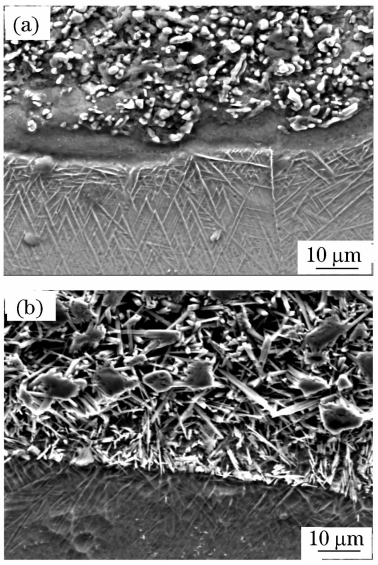

Fig. 8. SEM micrographs of the interface between the coating and the substrate. (a) Cr_3C_2+Ti; (b) TiB_2+Ti.

The micrographs of the interface between the coating and the substrate are shown in Fig. 8. An excellent metallurgical bond exists between the coating and the substrate. It is worth noting that there is an apparent boundary between the substrate and Cr_3C_2+Ti coating (Fig. 8(a)), due to the planar growth in the bottom of the molten pool. In contrast, there is no an inter-gradation of planar crystal between TiB_2+Ti coating and the substrate (Fig. 8(b)).

3.3 Microhardness

The microhardness distribution of the coatings is shown in Fig. 9. The microhardness in the Cr_3C_2+Ti coating is high and has a sharp falling in the interface between the coating and the substrate. The microhardness

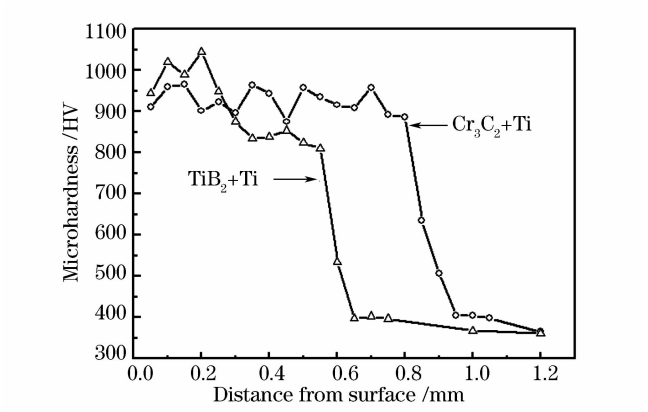

Fig. 9. Microhardness distribution of the coatings.

distribution in the TiB_2+Ti coating also shows a profile similar to that in the Cr_3C_2+Ti coating. The microhardnesses are approximately HV850∼HV1000 and HV800∼HV1050 in the Cr_3C_2+Ti and TiB_2+Ti coating, respectively. The average microhardness of substrate is HV360. The microhardness of the coatings is 2 ∼ 3 times higher than that of Ti-6Al-4V substrate.

4. Conclusions

In Cr_3C_2+Ti laser clad coating, the Cr_3C_2 particles are completely dissolved and then deposited to form dendritic and spherical TiC in the clad coating. In TiB_2+Ti laser clad coating, most TiB_2 particles are dissolved and then deposited to form TiB which is present of coarse and fine needles. Meanwhile a few quasi-melted TiB_2 particles surrounded by TiB particles were observed in the bottom of coating. The microhardnesses are approximately HV850∼HV1000 and HV800∼HV1050 in the Cr_3C_2+Ti and TiB_2+Ti coatings, respectively. The microhardness of the coatings is 2 ∼ 3 times higher than that of Ti-6Al-4V substrate.

This work was supported by China Postdoctoral Science Foundation (No. 20060400700) and Tianjin Technology Development Foundation of Higher Education (No. 20060912). W. Niu's e-mail address is newways_2005 @126.com.

References

1. V. Ocelík, D. Matthews, and J. Th. M. De Hosson. Sliding wear resistance of metal matrix composite layers prepared by high power laser [J]. *Surface and Coatings Technology* **197,** 303 ∼ 315 (2005).
2. S. Mridha and T. N. Baker. Metal matrix composite layer formation with 3 pm SiCp powder on IM13 18 titanium alloy surfaces through laser treatment [J]. *J. Mater. Proc. Technol.* **63,** 432 ∼ 437 (1997).
3. W. L. Wu. Microstructure of TiC dendrites reinforced titanium matrix composite layer by laser cladding [J]. *J. Mater. Sci. Lett.* **22,** 1169 ∼ 1171 (2003).
4. B. J. Kooi, Y. T. Pei, J. Th. and M. De Hosson. The evolution of microstructure in a laser clad TiB-Ti composite coating [J]. *Acta Materialia* **51,** 831 ∼ 845 (2003).
5. Q. Meng, L. Geng, and D. Ni. Laser cladding NiCoCrAlY coating on Ti-6Al-4V [J]. *Mater. Lett.* **59,** 2774 ∼ 2777 (2005).
6. W. Zhang and Z. Liu. Study on microstructure of in-situ synthesis of TiC-Cr7C3-Ti-Ni metal-ceramics composite coating [J]. *Chinese J. Lasers* (in Chinese) **35,** 1091 ∼ 1094 (2008).
7. W. Wang, F. Sun, and M. Wang. Wang Maocai. Laser cladding Ni-based Tribaloy 700 coatings on TA2 titanium alloy [J]. *Chinese J. Lasers* (in Chinese) **34,** 1710 ∼ 1715 (2007).
8. A. Cui, F. Hu, and L. Hui. Microstructure and wear-resisting property of (Ti+Al/Ni)/ (Cr_2O_3+CeO_2) laser cladding on titanium alloy [J]. *Chinese J. Lasers* (in Chinese) **34,** 438 ∼ 441 (2007).